Missouri University of Science and Technology

Scholars' Mine

International Specialty Conference on Cold-Formed Steel Structures

(1973) - 2nd International Specialty Conference on Cold-Formed Steel Structures

Oct 22nd, 12:00 AM

Nonlinear Analysis of Thin-walled Continuous Beams

Shien T. Wang

Follow this and additional works at: https://scholarsmine.mst.edu/isccss

 Part of the Structural Engineering Commons

Recommended Citation

Wang, Shien T., "Nonlinear Analysis of Thin-walled Continuous Beams" (1973). *International Specialty Conference on Cold-Formed Steel Structures*. 1.
https://scholarsmine.mst.edu/isccss/2iccfss/2iccfss-session3/1

This Article - Conference proceedings is brought to you for free and open access by Scholars' Mine. It has been accepted for inclusion in International Specialty Conference on Cold-Formed Steel Structures by an authorized administrator of Scholars' Mine. This work is protected by U. S. Copyright Law. Unauthorized use including reproduction for redistribution requires the permission of the copyright holder. For more information, please contact scholarsmine@mst.edu.

NONLINEAR ANALYSIS OF THIN-WALLED CONTINUOUS BEAMS

Shien T. Wang[1], A.M. ASCE

INTRODUCTION

Thin-walled cold-formed steel continuous beams have been widely used in load carrying structures and other areas of application in recent years. Due to the large width-thickness ratio of the compression elements encountered in thin-walled beams, the buckling and post-local-buckling behavior of these elements is of major concern in the analysis of these members. The basic concept underlying the design of these members involves the utilization of the post-buckling strength of the compression elements which comprise the cross-sections of these members.

The available post-buckling strength in these thin compression elements can be accounted for by the concept of effective width which has been well established in light-gage steel design (1, 2). A typical cold-formed corrugated cross-section of a beam subjected to a positive or negative moment is shown in Fig. 1(a). The effective width concept of a buckled compression element is shown in Fig. 1 (b). With this concept, first proposed by Von Karman (8), the nonuniform stress distribution over the full width w of the compression element after buckling is replaced by an equivalent uniform stress distribution, equal in intensity to the edge stress σ_{max} of the compression element, but applied over an effective width b. The total load carried by the element is the same in both distributions. This post-buckling behavior and the concept of effective width introduce nonlinearities in the response of thin-walled sections and necessitate an iterative type analysis procedure.

On the other hand, for cold-formed sections the material response may be inelastic, which may be nonlinear originally or as a result of cold-rolling

[1]Asst. Prof. of Civ. Engrg., Univ. of Kentucky, Lexington, Ky.

or cold-forming process. Because of this process, nonuniform material response across the cross-section (Fig. 2) may also occur (12).

Both the above factors lead to a nonlinear moment-curvature relation for an element of the beam. Since the effective width of the compression element decreases as the stress borne by the compression element edge increases, the effective flexural stiffness of the cross-section varies along the beam depending upon the magnitude of the moment at the section. The direct approach of the approximate analysis of the problem is to consider the moment-curvature relationship of the beam (10, 12). Based on this concept, a discrete mathematical model was used by Wang, Winter, and Errera (9, 11) in the analysis of thin-walled simple beams using numerical integration techniques.

For continuous beams, it is further complicated by the fact that the bending moment distribution along the beam is not known a priori due to the interdependence of beam stiffness and the moment distribution of the beam. This problem was discussed in a paper by Bleustein and Gjelsvik (3) for two-span thin-walled beams. More recently, Wang (12) has extended the numerical method used earlier (9) to two-span continuous beams. For multi-span continuous beams, the compatibility conditions at all supports must be satisfied and the problem becomes more involved. Research on this subject is urgently needed.

It is the purpose of this paper to present a method for the post-buckling analysis of thin-walled multi-span continuous beams. The proposed method is employed to analyze the beams subjected to several typical loading and support conditions. Effects of shapes of the moment-curvature relations on the behavior of beams are studied. Both stainless steel and carbon steel beams are considered. Convergence characteristics of the proposed solution scheme are investigated. Finally, simplified methods for deflection predictions, which may be adopted for design use, are presented.

METHOD OF ANALYSIS

The rigorous solution to the problem of predicting the flexural behavior of thin-walled continuous beams must treat the buckling and post-buckling behavior of the compression elements and their interaction with the other elements of the section as well as the compatibility conditions at all supports. Owing to the complexity involved, only a simple case, i.e. simply supported lipped channel beams subjected to equal end moments, has been considered by Rhodes and Harvey (7). The results obtained by them showed good agreement with those obtained by using Winter's equation (1,13), which is an experimental modification of Karman's effective width expression. In view of the material characteristics as well as the support and loading conditions for the problem being considered, such an analysis is extremely complex.

In this paper, a numerical method is presented by utilizing the effective width concept to account for the post-buckling strength of the buckled compression elements of the beam. This concept has been used successfully in the previous studies of thin-walled beams subjected to static and impact loads (5, 9, 11, 12, 16).

Moment-Curvature Relationship. - A numerical approach was used by the author in the previous studies (9,11,12) to compute the moment-curvature data with the aid of the effective width concept. Using numerical integration and the equation of internal equilibrium, the internal moment and the corresponding curvature can be computed by the plane section assumption. The same method is employed in this study to generate the moment-curvature data for the sections considered. The nonlinear stress-strain curves shown in Fig. 2 are approximated by the Ramberg-Osgood formula (9). The following Winter's effective width equation (1) is used to account for the post-

buckling strength of the compression elements of the beams.

$$\frac{b}{t} = 1.9\sqrt{\frac{E}{\sigma_{max}}}\left(1 - 0.415\ \frac{t}{w}\sqrt{\frac{E}{\sigma_{max}}}\right) \qquad (1)$$

when $\frac{w}{t} \geq 1.288\sqrt{\frac{E}{\sigma_{max}}}$, in which b = effective width of the compression element stiffened along both unloaded edges; t = thickness; E = modulus of elasticity in compression; w = flat width of the compression element; and σ_{max} = edge stress. For values smaller than $1.288\sqrt{\frac{E}{\sigma_{max}}}$, b= w.

Using this numerical procedure and the stress-strain curves shown in Fig. 2, the typical moment-curvature relationship of a hat section (Section 1B) which has compact bottom flanges subjected to the positive and negative moments was obtained and are shown in Fig. 3, (12).

Nonbuckling Analysis.- A portion of a continuous beam with an arbitrary loading is shown in Fig. 4(a) for the purpose of illustration of the proposed method of analysis. The negative moment at each interior support, M_i, is taken as a redundant. For an elastic prismatic beam based on the flexibility method of analysis, the following equation results (4)

$$\left[f\right]\ \left\{M\right\} = -6EI\ \left\{D\right\} \qquad (2)$$

in which $\left[f\right]$ = flexibility matrix of the released structure multiplied by 6EI; $\left\{M\right\}$ = column matrix of unknown moments at supports; $\left\{D\right\}$ = column matrix of the relative rotation at each support of the released structure due to external loading or to the various effects combined; and EI=flexural rigidity of the beam. The ith equation of Eq. 2 can be written as

$$M_{i-1}\ \ell_i + 2M_i\ (\ell_i + \ell_{i+1}) + M_{i+1}\ell_{i+1} = -6EI\ D_i \qquad (3)$$

in which ℓ_i and ℓ_{i+1} are the span length to the left and right of support i, respectively; M_i is the unknown moment at support i; and D_i is the relative rotation at support i as defined above. The expression is also known as the equation of three moments.

This simple elastic nonbuckling analysis of the beam leads to a moment diagram $\{M\}_{j=1}$, as shown in Fig. 4(b). This moment distribution is used as the first trial in the direct iterative procedure for the post-buckling analysis of the continuous beam. The subscript j indicates the cycle of iteration.

Post Buckling Analysis.- The discrete mathematical model used in the earlier studies by the author (9,11,12) is used here for the post-buckling analysis. For the discrete model, the continuously flexible beam is replaced with a finite number of rigid elements connected by flexible joints at which the continuously varied curvature is lumped using a numerical integration procedure. Based on the moment distribution obtained in the nonbuckling analysis, $\{M\}_{j=i}$, the moment at each node of the idealized discrete mathematical model is determined and the corresponding curvature can be obtained through interpolation of the moment-curvature data calculated. Considering the compatibility conditions at supports and using Newmark's numerical integration procedure (6), the slopes at both ends of each span are obtained separately. The angle gap $(\Delta\theta_i)_j$ at support i due to the relative rotation of adjacent beam ends is given as

$$(\Delta\theta_i)_j = (\theta_i)_j + (\theta_i')_j \qquad (4)$$

in which θ_i and θ_i' are the computed slopes at the end of the spans to the left and right of support i, respectively, as shown in Fig. 4(c). The

resulting angle gaps at the supports are due to the fact that the assumed moment distribution based on the elastic nonbuckling analysis is not the true one. Based on the computed angle gaps, the moment diagram is adjusted and the procedure is repeated.

In view of the nonlinear nature of the moment-curvature relationship of the beam, the following procedure is proposed. After the angle gaps are computed based on the trial moment distribution (j=1), the next trial moment distribution (j+1) is shown in Fig. 4(b). The shaded area is the estimated correction moment distribution, also shown in the same form in Fig. 4(d), which is required by the compatibility condition at the supports. The required correction moment at supports, ΔM_i, may be estimated by the following equation by assuming that the buckled beam is elastic prismatic with an equivalent constant stiffness $(EI)_{eqv}$

$$\left[f \right] \left\{ \frac{\Delta M}{(EI)_{eqv}} \right\}_j = -6 \left\{ \Delta\theta \right\}_j \tag{5}$$

in which $\left[f \right]$ is the same coefficient matrix in Eq. 2; $\left\{ \frac{\Delta M}{(EI)_{eqv}} \right\}_j$ is a column matrix of the required correction moment at each support divided by the equivalent constant stiffness; and $\left\{ \Delta\theta \right\}_j$ is a column matrix of the computed angle gap at each support. Eq. 5 can also be written in terms of curvature as

$$\left[f \right] \left\{ \Delta\phi \right\}_j = -6 \left\{ \Delta\theta \right\}_j \tag{6}$$

in which $\left\{ \Delta\phi \right\}_j$ is a column matrix of the required corrections of curvature at supports for the assumed equivalent elastic prismatic beam.

If the calculated $(\Delta\theta_i)_j$ at each support is less than a predescribed tolerance (10^{-5} rad.) or a predetermined number of iteration (j=30) is reached, the procedure is completed. Otherwise, the adjusted moment at

the supports, $\{M\}_{j+1}$, are computed from the moment-curvature data by interpolation from the following general expression.

$$\{\phi\}_{j+1} = \{\phi\}_j + \xi \{\Delta\phi\}_j \qquad (7)$$

in which $\{\phi\}_{j+1}$ is a column matrix of the adjusted curvatures at the supports; $\{\phi\}_j$ is a column matrix of curvatures at supports corresponding to $\{M\}_j$; and ξ is a correction factor to accelerate the convergence procedure. The use of a correction factor in the above equation is theoretically justified since by assuming an equivalent constant stiffness throughout the buckled continuous beam , the computed $\Delta\phi_i$ may underestimate or overestimate the required correction depending on the relative effective stiffnesses of the beam in the positive and negative moment zones. This procedure is considered to be necessary because of the nonlinear nature of the moment-curvature relations of the beam in the post-buckling range. It is, therefore, necessary to investigate the convergence characteristics of the proposed procedure and to determine the range of correction factors for which rapid convergence can be achieved. A computer program following this solution scheme has been developed to perform the entire calculation(14).

CONVERGENCE CRITERIA

Two types of moment-curvature relations as shown in Fig. 3 are considered to investigate the convergence characteristics of the proposed method. The unsymmetrical case is represented by Section 1B, while the symmetrical case is represented by a fictitious section, Section 1A. The loading and support conditions considered are Cases 1 and 4 shown in Fig. 5.

The results of this study are shown in Fig. 6 . In general, the convergence

characteristics of multi-span beams are similar to the earlier study on two -span beams (12). However, the oscillating and non-oscillating type convergence characteristics are no longer predictable because of the interaction of multi-spans unless a fairly small correction factor is used. For the same reason, the range of the applicable correction factor is narrower than the previous case. At the optimum ξ, the required numberof iterations for convergence in this case is also slightly more than that of a two-span beam.

As the magnitudeof the loading increases, the nonlinear effect becomes more pronounced. With a higher loading level, the number of iterations required for convergence is more than that for a lower loading level with the same correction factor except for Case 1 loading when a correction factor larger than the optimum value is used.

By examining the optimum value of ξ, it is seen that for Section 1A with symmetrical moment-curvature relationships, the optimum value of ξ is larger than that for Section 1B with unsymmetrical moment-curvature relationships.

Due to the interaction between the moment-curvature relations and the moment distribution along the beam, the loading condition will influence the convergence characteristics. It is noted that for Case 1 loading, the optimum value of ξ is slightly larger than that for Case 4 loading. On the other hand, the range of the applicable ξ is the widest for the section with symmetrical moment-curvature relations for an ordinary loading and support condition, i.e., Case 1.

Examining the data presented, it is concluded that with an appropriate selection of ξ, the proposed procedure converges rapidly and a solution is ensured. For all the cases investigated herein, it is seen that up to 12

iterations will be needed for a choice of the correction factors ranging from 0.4 to 1.1 for the case of unsymmetrical moment-curvature relationships, and from 0.8 to 1.5 for the symmetrical case. Correction factors ranging from 0.8 to 1.1 will result in a rapid convergence of less than 12 iterations for all the cases considered. This factor, especially the optimum value, is dependent on the moment-curvature characteristics of the beam, loading levels, and loading and support conditions.

The proposed solution scheme is rather general and can be applied to other sections as long as the slope of the moment-curvature curve of the section changes gradually. The procedure may not converge for loading levels approaching failure when the moment-curvature curve is flattened out rapidly. In this case, the procedure must be modified or an incremental method of analysis may be used.

POST-BUCKLING BEHAVIOR

In order to investigate the general behavior of beams with different configurations and loading conditions, three kinds of typical corrugated sections cold-formed from cold-rolled stainless steel and carbon steel are considered. The dimensions of these three sections are shown in Table 1 with reference to Fig. 1 (a). They represent three typical cases of symmetrical and unsymmetrical moment-curvature relationships. The moment-curvature relations of the stainless steel sections based on the material properties presented in Fig. 2 are shown in Fig. 7. The moment-curvature relations of the sectionsbased on the elasto-plastic as well as the linearly elastic stress-strain relationships are shown in the same figure. The modulus of elasticity and the yield stress for the carbon steel are taken as 29.5×10^3 ksi and 50 ksi, respectively. Loading and support conditions considered are shown in Fig. 5. These sections and loading conditions represent a wide range of applications.

In applying the proposed procedure to these cases, each span was divided into 20 segments for the discrete model. Several loading levels were selected to cover a wide range of response in the post-buckling domain. The complete moment-curvature relationship for each section is represented by 180 data points.

Moment Distribution (Stainless Steel Beams). - The computed moments at supports, M_1, for Cases 1 and 4 loading are compared with those of an elastic prismatic beam in Table 2. The absolute values of the deviations of the computed moments from those of a prismatic beam based on the elastic nonbuckling analysis increase with the increasing loading level for all the cases considered.

For Case 1 loading, which is commonly encountered in practice, the computed actual moments are very close to those based on the elastic prismatic beam. The signs of the deviation are all negative for Section 2A which possesses symmetrical moment-curvature relationships. This is due to the fact that the reduction in stiffness in the negative moment zones is more pronounced than that for the positive moment zones of the beam. For Section 2B, the signs of the deviation are mixed because of the interaction between the unsymmetrical moment-curvature relations of the section and the bending moment distribution along the beam. Since the moment-curvature relationship of Section 2C is the reverse of Section 2B, the deviations of Section 2A are between those of Sections 2B and 2C. The deviations for Case 2 loading are even smaller because of the uniformity in loading and support conditions.

For Case 4 loading, all three sections show certain deviations with mixed signs. This is due to the interaction between the characteristics of the moment-curvature relationship of the beam and the irregular moment

distribution along the beam. Due to this interaction, the trend of the variation of deviation becomes rather difficult to predict. For Case 3 loading, a similar situation is encountered.

Moment Distribution (Carbon Steel Beams). - By examining Fig. 7, it is seen that the moment-curvature curves of carbon steel sections start to flatten out rapidly after the sections begin to yield. The convergence characteristics for carbon steel beams are similar to stailess steel beams in the initial stage. When the beam is loaded beyond the yield stress, the required number of iterations for convergence increases sharply. This is due to the fact that the moment distribution of an elastic prismatic beam is used as the first trial and in this post-yielding range a small change in moment may cause a very large change in curvature. The highest loading level considered for each section (Table3) results in a moment corresponding to a partially yielded section at one or more supports. With an even higher load, the procedure may not converge.

By comparing the results shown in Table3 with those in Table 2, similar conclusions for stainless steel beams also apply to carbon steel beams. The deviations of the actual moments from those of an elastic prismatic beam are much smaller for the carbon steel beams due to the less pronounced nonlinear effect and unsymmetry of the moment-curvature relationships of the carbon steel section than the stainless steel section. However, these deviations may be slightly larger for beams made of carbon steels with yield stresses higher than 50 ksi used since the nonlinearity due to local buckling will be more pronounced at a higher stress level.

Based on the preceding discussion, it is noted that the actual moment distribution of the continuous beam in the post-buckling range is dependent on moment-curvature relations, loading levels, and loading and support

conditions. The increase or decrease of the moments at the supports from the moments based on the nonbuckling analysis depends on the interaction of the above factors. For a beam with symmetrical moment-curvature relationships subjected to an ordinary loading and support conditions, such as Case 1, the actual moment distribution is very close to that of an elastic prismatic beam. For beams with unsymmetrical moment-curvature relationships, especially for those with large differences in positive and negative moments, subjected to irregular loading and support conditions, the discrepancy between the actual moment distribution and that obtained by the nonbuckling analysis could be appreciable for stainless steel beams (±15% and ± 25% for Cases IV and III loading, respectively). In these cases, the nonlinear effects due to local buckling and material characteristics should be considered in the analysis. However, if only an approximate analysis is required, the computed moments based on the elastic prismatic beam assumption may be used. This is especially true for carbcn steel beams.

Deflection.- The deflection at each node of the discrete model is obtained from the last cycle of iteration. The deflection converges rapidly as the number of segments of the idealized beam increases. The location of maximum deflection at each loading level will change depending on the moment distribution and the variation of the beam stiffness, although the amount of shifting may be very small. The maximum deflections for the three stainless steel sections considered are shown in Table 4 for Cases 1 and 4 loading. The maximum deflection occurs in the end span for Case 1 loading. The moment-curvature relationships for Section 2A are the strongest among those of three sections for both the positive and negative moments, therefore, the deflection

of Section 2A is less than that of the other two sections. The relative magnitude of deflection for sections 2 B and 2C depends on the interaction between the moment distribution along the beam and the moment-curvature relationships of the sections.

SIMPLIFIED METHODS FOR DESIGN

Moment Distribution. -Since the actual moment distribution is not appreciably different from that of an elastic prismatic beam except for a few cases, this suggests that for an approximation, the moment distribution based on the nonbuckling analysis may be used for selecting a section. This is especially appropriate for carbon steel beams and for stainless steel beams with symmetrical moment-curvature relations subjected to an ordinary loading and support condition. This simplification would eliminate most of the numerical calculations involved in the iterative procedure for finding the actual moment distribution of the beam for the given loading condition.

Simplified Model. - It has been found in this study as well as the earlier study (12) that only a few segments of the discrete model were required to achieve a reasonable accuracy for deflection predictions. Recognizing the variations of the effective stiffnesses in the positive and negative moment zones, it is proposed for a simplified model to divide the beam into a number of segments in each of which the bending moment has the same sign. For each of these segments a single reduced effective constant stiffness based on the maximum moment in that segment can be computed. The overall beam is thus considered as built up of segments in each of which the stiffness is a constant. A typical span of a continuous beam is shown in Fig. 8 (a). Two of the possible idealized discrete models of the span are shown in Fig. 8, (c) and (d), depending on the moment-curvature

characteristics of the section and the magnitude of the negative moments. A similar idealization for two-span beams was considered by Bleustein and Gjelsvik (3) and Wang (12).

Simplified Methods for Deflection Determination.

Method I: In the model, the segments are brought together by the compatibility conditions at the junctions of any two segments. The governing equations for the deflection of the model were derived in terms of the effective stiffnesses and the locations of the boundaries of the segments and the end moments (14). The maximum deflection of the idealized beam is then computed.

Method II: Although the above method provides a rigorous approach for deflection predications of the idealized beam, it still requires considerable amount of computation. The simplest approach is to use a constant effective stiffness $(EI)_{avg}$ throughout the beam, which is an average of the stiffnesses of all the segements. Similar idea is used in concrete design as discussed by Yu (15). In this case, the ordinary deflection equation of an elastic prismatic beam can be used. This proposition greatly simplifies the calculations.

Method III: It should be noted that Method II does not take into account the length and location of segments of the idealized beam. In order to improve the accuracy of Method II, it is proposed to use the average of the segment stiffnesses weighted linearly according to their respective lengths. In this case, the length effect is considered and, on the other hand, the simplicity of using the deflection equation of an elastic prismatic beam is retained.

Comparison of Results: Using the above simplified methods, the computed maximum deflection of stainless steel beams for the cases considered are

compared with the results from the numerical method described earlier in this paper in Table 4. The degree of inaccuracy is seen to increase with the increase of the loading magnitude in all the cases considered.

The inaccuracy of Method I is caused by the minimum constant stiffness assumption in each segment and the use of moment distribution of an elastic prismatic beam based on the nonbuckling analysis. If the actual moment distribution were used, the computed deflection would be always on the conservative side, i.e. larger than the actual deflection of the original beam. Since the moment distribution of an elastic prismatic beam is used, the computed deflection may be conservative or unconservative depending on the loading condition and the moment-curvature relations of the beam.

The discrepancy of Method II is further caused by neglecting the effects of length and location of each segment. The degree of inaccuracy of Method III falls between the first two methods, as expected.

For carbon steel beams, the degree of inaccuracy of these methods are similar to that of stainless steel beams just described. However, the computed deflections are more conservative than those of stainless steel beams since the actual moment distribution of carbon steel beams are closer to those based on the elastic nonbuckling analysis. Based on this study, it seems that both Methods II and III are simple with acceptable accuracy. Method III is especially a suitable method which yields not only results with acceptable accuracy but also on the conservative side for the typical cases investigated. Although the methods discussed are approximate in nature, they do provide the engineer with a simple way to estimate deflections with reasonable accuracy. In fact, these methods are within the spirit of the current design codes (1, 2, 15). The proposed approach of using the reduced

effective stiffness concept is of special advantage particularly for beams with nonlinear material properties.

CONCLUSIONS

A numerical method has been presented for predicting the post-buckling response of thin-walled continuous beams. Nonlinearities due to local buckling and nonlinear material characteristics are accounted for by the nonlinear moment-curvature relations of a section derived with the aid of the effective width concept. The proposed method includes a numerical integration procedure in conjunction with the flexibility matrix method of analysis. Using the moment distribution of an elastic prismatic beam based on the nonbuckling analysis as a first approximation, convergence of the procedure has been found to be dependent on the moment-curvature relations of beam sections, loading levels, and the loading and support conditions. It has been shown that with an appropriate selection of the correction factor, the numerical iterative procedure converges rapidly.

For the typical cases considered, it has been found that the actual moment distribution of the beam in the post-buckling range is close to that of an elastic prismatic beam except for the cases when the moment-curvature relation for the positive moment is appreciably different from that for the negative moment and when the loading and support condition of the beam is somewhat irregular.

Simplified methods for predicting deflections in the post-buckling range are formulated based on the concept of the reduced effective stiffnesses. Using a weighted single constant reduced stiffness based on the stiffnesses derived from the maximum positive and negative moments of an elastic prismatic beam, the ordinary beam deflection equation can be used for

computing deflections with acceptable accuracy.

Since the techniques presented are quite general, the method can be used for other similar problems. Experimental verification would be very helpful to further confirm the suitability of the method presented.

ACKNOWLEDGMENTS

The study reported herein was supported in part by the University of Kentucky through a Faculty Research Fellowship. The assistance of S. S. Yeh, graduate assistant, in deriving and obtaining some of the results presented herein is gratefully acknowledged. The support given by the University of Kentucky Computing Center for the use of IBM 360 computer is appreciated.

APPENDIX I. - REFERENCES

1. American Iron and Steel Institute, "Specification for the Design of Cold-Formed Steel Structural Members," New York, N.Y., 1968; and Winter, G., "Commentary on the Specification for the Design of Cold-Formed Steel Structural Members,", 1970.

2. American Iron and Steel Institute, "Design of Light-Gage Cold-Formed Stainless Steel Structural Members," New York, N.Y., 1968.

3. Bleustein, J. L., and Gjelsvik, A., "Rational Design of Light Gage Beams," Journal of the Structural Division, ASCE, Vol. 96, No. ST7, July, 1970, pp. 1535-1541.

4. Ghali, A., and Neville, A.M., Structural Analysis: A Unified Classical and Matrix Approach, International Textbook Co., Scranton, Pa., 1972.

5. Johnson, A.L., and Winter, G., "Behavior of Stainless Steel Columns and Beams," Journal of the Structural Division, ASCE, Vol. 92, No. ST5, Oct., 1966, pp. 97-118.

6. Newmark, N. M., "Numerical Procedure for Computing Deflections, Moments, and Buckling Loads," Proceedings, ASCE, Vol. 68, 1942, pp. 691-718.

7. Rhodes, J., and Harvey, J.M., "The Local Buckling and Post Local Buckling Behavior of Thin-Walled Beams," Aeronautical Quarterly, Vol. XXII, Nov. 1971, pp. 363-388.

8. Von Karman, T., Sechler, E.E., and Donnell, L. H., "The Strength of Thin Plates in Compression," Transactions, ASME, Vol. 54, 1932, pp. 53-57.

9. Wang, S.T., and Winter, G., "Cold-Rolled Austenitic Stainless Steel: Material Properties and Structural Performance," Report No. 334, Department of Structural Engineering, Cornell University, Ithaca, N.Y., July, 1969.

10. Wang, S.T., Discussion on "Rational Design of Light Gage Beams," by Bleustein, J.L. and Gjelsvik, A., Journal of the Structural Division, ASCE, Vol. 97, No. ST5, May, 1971, pp. 1639-1641.

11. Wang, S.T. and Errera, S.J., "Behavior of Cold-Rolled Stainless Steel Members," Proceedings of the First Specialty Conference on Cold-Formed Steel Structures, University of Missouri- Rolla, Rolla, Missouri, Aug., 1971.

12. Wang, S.T., "Post-Buckling Behavior of Cold-Formed Thin-Walled Stainless Steel Beams," International Journal of Computers and Structures, in press.

13. Winter, G., "Strength of Thin Steel Compression Flanges," Transactions, ASCE, Vol. 112, 1947, Also in Cornell University Experimental Station, Reprint No. 32, Oct., 1947.

14. Yeh, S.S., "Post-Buckling Behavior of Thin-Walled Continuous Beams," thesis presented to the University of Kentucky, Lexington, Kentucky in 1973, in partial fulfillment of the requirements for the degree of Master of Science.

15. Yu, W.W., Discussion on "Rational Design of Light Gage Beams," by Bleustein, J.L. and Gjelsvik, A., Journal of the Structural Division, ASCE, vol. 96, no. ST12, Dec., 1970.

16. Zanoni, E.A., and Culver, C.G., "Impact Loading of Thin-Walled Beams," Proceedings of the First Specialty Conference on Cold-Formed Steel Structures, University of Missouri - Rolla, Rolla, Missouri, Aug., 1971.

APPENDIX II. - NOTATION

The following symbols are used in this paper:

B_1, B_2	=	flat width of α and β flanges, respectively;
b	=	effective width of compression element;
b_1, b_2	=	effective width of α and β flanges under compression, respectively;
D	=	depth of corrugated section;
E	=	modulus of elasticity in compression;
$\{D\}$	=	column matrix of relative rotation at each support of the released structure due to external loading or the various effects combined;
$(EI)_{eqv}$	=	equivalent constant stiffness;
$(EI)_k$	=	minimum constant stiffness of region k of a beam;
$(EI)_{avg}$	=	flat or weighted average stiffness;
$[f]$	=	flexibility matrix of the released structure multiplied by 6EI;

i	=	support number;
j	=	number of iteration;
ℓ_i	=	span length to the left of support i;
M_i	=	negative moment at support i;
$\{M\}$	=	column matrix of moment at each support;
R	=	inside radius;
t	=	thickness;
w	=	uniformly distributed load in lb./in.;
w_1, w_2	=	flat width of α and β flanges exclusive of fillets;
ΔM_i	=	correction moment at support i;
$\Delta\theta_i$	=	angle gap at support i;
$\{\Delta\theta\}$	=	column matrix of angle gap at each support;
$\{\Delta\phi\}$	=	column matrix of the required curvature correction at each support;
$(\theta_i), (\theta_i')$	=	computed slopes to the left and right of support i, respectively;
ε	=	correction factor;
σ_{max}	=	maximum edge stress; and
$\{\phi\}$	=	column matrix of curvature at each support.

TABLE 1.- BEAM SECTION DIMENSIONS

Dimensions	Sections		
	2 A	2 B	2 C
	(2)	(3)	(4)
B_1, in in.	2.5492	2.5492	0.8764
D_1, in in.	1.5000	1.5000	1.5000
B_2 in in.	2.5492	0.8764	2.5492
R, in in.	0.0938	0.0938	0.0938
t, in in.	0.0328	0.0328	0.0328
R/t	2.86	2.86	2.86
w_1/t	70.00	70.00	19.00
w_2/t	70.00	19.00	70.00

TABLE 2. - MOMENT AT SUPPORT - STAINLESS STEEL BEAMS

Loading Case	Support No.	Load w	Moment of Elastic Prismatic Beam	Section 2A - SS		Section 2B - SS		Section 2C - SS	
				Actual Moment	Deviation (5)-(4) / (4)	Actual Moment	Deviation (7)-(4) / (4)	Actual Moment	Deviation (9)-(4) / (4)
		in lb/in.	in in.-lb.	in in.-lb.		in in.-lb.		in in.-lb.	
(1)	(2)	(3)	(4)	(5)	(6)	(7)	(8)	(9)	(10)
Case 1	1	20	-4148.57	-4088.42	- 1.45%	-4224.58	+ 1.83%	-3988.93	-3.85%
	2		-2765.71	-2748.89	- 0.61%	-2721.18	- 1.61%	-2787.32	+0.78%
	1	30	-6222.85	-6100.66	- 1.96%	-6409.96	+ 3.01%	-5844 21	-6.09%
	2		-4148.55	-4106.22	- 1.02%	-4073.00	- 1.82%	-4158.63	+0.26%
	1	40	-8297.14	-8091.04	- 2.48%	-8608.10	+ 3.75%	-7633.87	-8.00%
	2		-5531.42	-5464.99	- 1.20%	-5426.29	- 1.97%	-5512.41	-0.34%
Case 4	1	20	- 921.90	997.75	+ 8.23%	- 964.19	+ 4.59%	- 982.16	+6.54%
	2		-1613.33	-1674.98	+ 3.83%	-1698.63	+ 5.29%	-1606.63	-0.42%
	3		-2304.76	-2353.34	+ 2.11%	-2401.44	+ 4.20%	-2276.30	-1.24%
	4		+1152.38	+1186.98	- 3.00%	+1205.97	- 4.65%	+1147.69	+0.4%
	5		-4379.04	-4238.92	- 3.20%	-4396.01	+ 0.39%	-4165.46	-4.88%
	1	30	-1382.85	-1550.08	+12.09%	-1523.22	+10.15%	-1483.27	+7.26%
	2		-2419.99	-2533.17	+ 4.68%	-2641.78	+ 1.73%	-2371.64	-2.00%
	3		-3457.14	-3561.31	+ 3.01%	-3702.85	+ 7.11%	-3370.70	-2.50%
	4		+1728.57	+1818.06	- 5.18%	-1846.50	- 6.82%	+1730.86	-0.13%
	5		-6568.57	-6280.38	- 4.39%	-6604.24	+ 0.54%	-6071.56	-7.57%
	1	40	-1843.80	-2115.43	+14.73%	-2134.57	+15.77%	-1995.99	+8.25%
	2		-3226.66	-3405.43	+ 5.54%	-3627.47	+12.42%	-3137.88	-2.75%
	3		-4609.52	-4780.17	+ 3.70%	-5045.47	+ 9.46%	-4460.88	-3.23%
	4		+2304.76	+2457.58	- 6.63%	-2492.55	- 8.15%	+2334.18	-1.28%
	5		-8758.29	-8281.95	- 5.44%	-8775.36	+ 0.20%	-7889.71	-9.92%

TABLE 3. - MOMENT AT SUPPORT - CARBON STEEL BEAMS

Loading Case	Support No.	Load w	Moment of Elastic Prismatic Beam	Section 2A -EP		Section 2B - EP		Section 2C - EP	
				Actual Moment	Deviation (5) - (4) / (4)	Actual Moment	Deviation (7) - (4) / (4)	Actual Moment	Deviation (9) - (4) / (4)
		in lb./in.	in in.-lb.	in in.-lb.		in in.-lb.		in in.-lb.	
(1)	(2)	(3)	(4)	(5)	(6)	(7)	(8)	(9)	(10)
Case 1	1	10	-2074.29	-2065.71	-0.41%	-2079.18	+0.24%	-2057.67	-0.80%
	2		-1382.85	-1385.88	+0.20%	-1380.43	-0.18%	-1389.67	+0.49%
	1	18	-3733.71	-3695.50	-1.02%	-3789.86	+1.50%	-3609.00	-3.34%
	2		-2489.14	-2482.42	-0.27%	-2461.26	-1.12%	-2518.83	+1.19%
	1	27	-5600.56	-5479.35	-2.16%	--	--	--	--
	2		-3733.71	-3725.63	-0.22%	--	--	--	--
Case 4	1	10	-2189.52	-2174.88	-0.67%	-2190.05	+0.02%	-2168.39	-0.97%
	2		-460.95	-465.12	+0.90%	-459.86	-0.24%	-466.51	+1.21%
	3		-806.67	-807.81	+0.14%	-810.36	+0.46%	-805.16	-0.19%
	4		-1152.38	-1155.12	+0.24%	-1155.88	+0.30%	+1152.80	+0.04%
	5		-576.19	+577.58	+0.24%	+577.93	+0.30%	+576.39	+0.03%
	1	18	-3941.14	-3852.64	-2.25%	-3954.80	+0.35%	+3773.16	-4.26%
	2		-829.71	-869.81	+4.83%	-850.96	+2.56%	-871.34	+5.02%
	3		-1452.00	-1491.47	+2.72%	-1502.42	+3.47%	-1440.34	-0.80%
	4		-2074.28	-2105.11	+1.49%	-2135.33	+2.94%	-2047.51	-1.29%
	5		+1037.14	+1055.48	+1.77%	+1067.67	+2.94%	+1028.11	-0.87%
	1	27	-5911.71	-5655.49	-4.33%	--	--	--	--
	2		-1244.57	-1377.40	+10.67%	--	--	--	--
	3		-2178.00	-2250.35	+3.32%	--	--	--	--
	4		-3111.43	-3180.40	+2.22%	--	--	--	--
	5		+1555.71	+1611.93	+3.61%	--	--	--	--

TABLE 4. - COMPARISON OF MAXIMUM DEFLECTIONS COMPUTED BY SIMPLIFIED METHODS - STAINLESS STEEL BEAMS

Loading Case	Section	Load w in lb./in.	Theoretical Deflection in in.	Method I		Method II		Method III	
				Deflection in in.	Deviation (5)-(4)/(2)	Deflection in in.	Deviation (7)-(4)/(4)	Deflection in in.	Deviation (9)-(4)/(4)
(1)	(2)	(3)	(4)	(5)	(6)	(7)	(8)	(9)	(10)
Case 1	2A - SS	20	0.1979	0.2004	1.30%	0.2106	6.45%	0.2053	3.74%
		30	0.3319	0.3372	1.61%	0.3614	8.89%	0.3486	5.04%
		40	0.4918	0.5009	1.84%	0.5490	11.62%	0.5234	6.42%
	2B - SS	20	0.3087	0.3271	5.96%	0.3107	0.63%	0.3191	3.35%
		30	0.5136	0.5605	9.13%	0.5216	1.55%	0.5413	5.39%
		40	0.7624	0.8555	12.21%	0.7868	3.20%	0.8214	7.74%
	2C - SS	20	0.2923	0.2772	-5.14%	0.3161	8.16%	0.2952	1.02%
		30	0.4689	0.4415	-5.84%	0.5337	13.82%	0.4836	3.13%
		40	0.6763	0.6244	-7.67%	0.8033	18.78%	0.7050	4.24%
Case 4	2A - SS	20	0.1914	0.2072	8.27%	0.1956	2.17%	0.2032	6.17%
		30	0.3187	0.3485	9.33%	0.3226	1.22%	0.3394	6.50%
		40	0.4621	0.5174	11.95%	0.4693	1.55%	0.5004	8.28%
	2B - SS	20	0.3067	0.3353	9.33%	0.3018	-1.59%	0.3227	5.22%
		30	0.4927	0.5718	16.05%	0.4784	-2.89%	0.5353	8.64%
		40	0.7045	0.8683	23.24%	0.6775	-3.84%	0.7908	12.25%
	2C - SS	20	0.2941	0.2942	0.02%	0.3025	2.83%	0.2975	1.15%
		30	0.4665	0.4646	-0.41%	0.4902	5.09%	0.4743	1.68%
		40	0.6617	0.6611	-0.09%	0.7072	6.88%	0.6786	2.55%

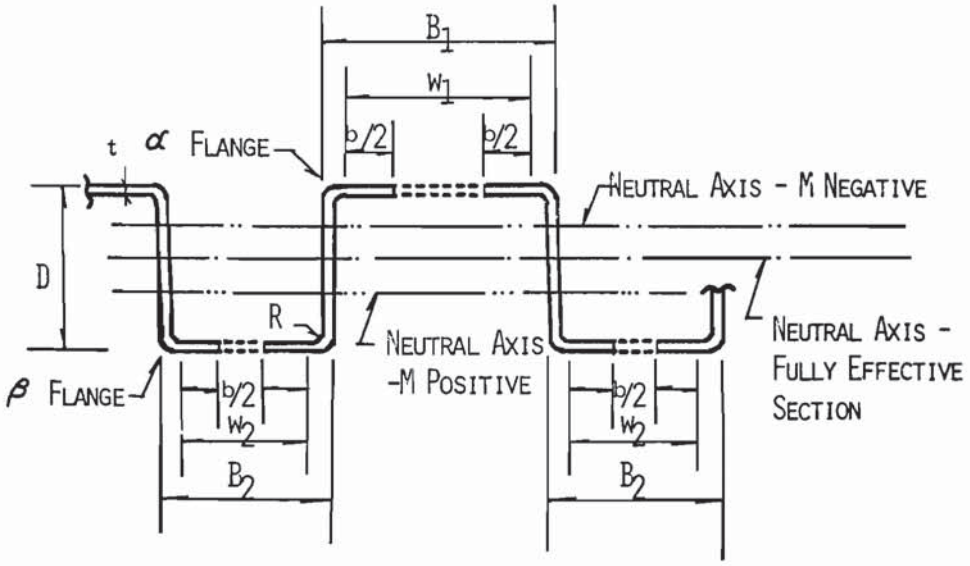

(a)

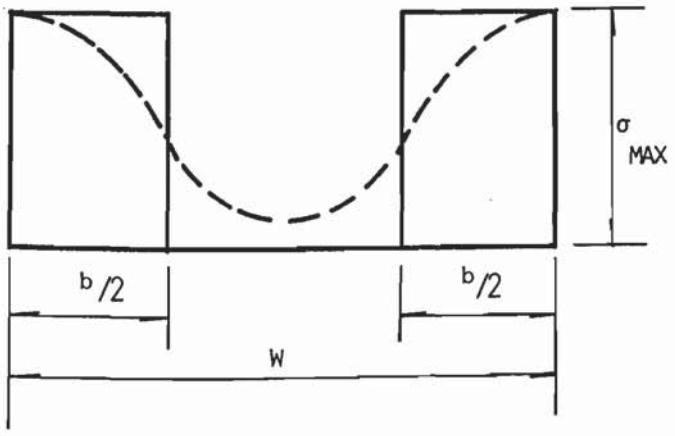

(b)

FIG. 1. - BUCKLED SECTION AND EFFECTIVE WIDTH CONCEPT

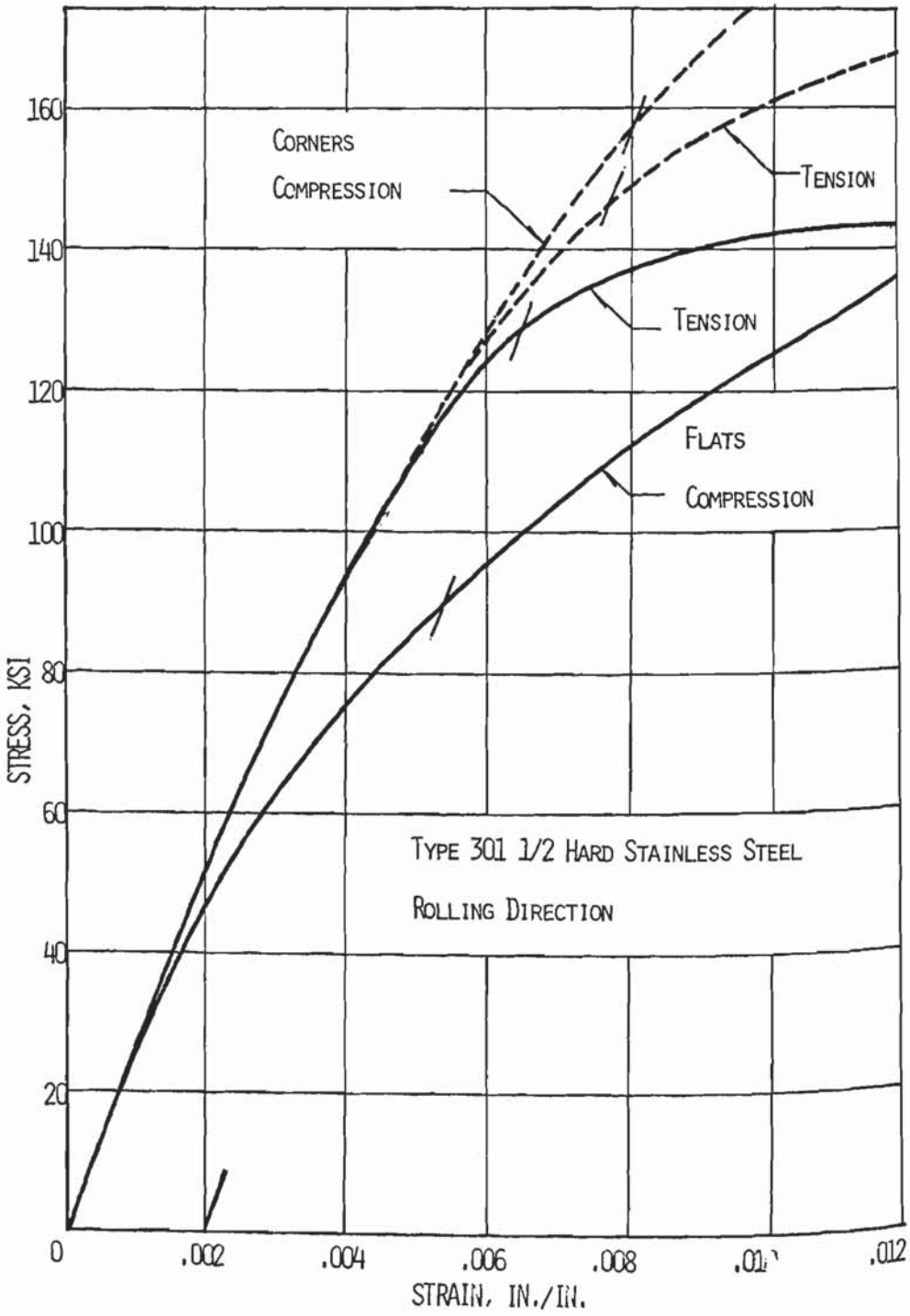

FIG. 2. -TYPICAL STRESS-STRAIN CURVES, FLATS AND CORNERS

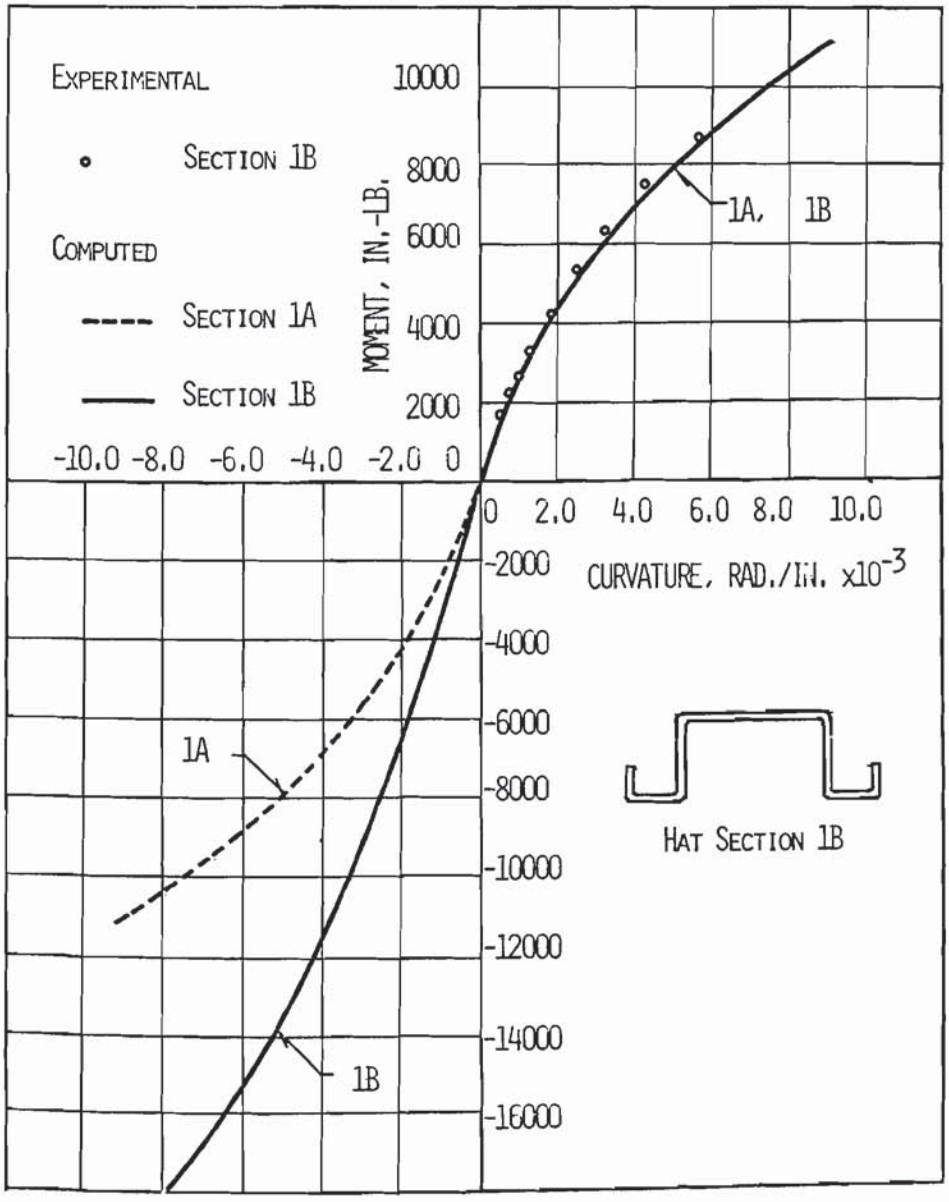

FIG. 3. - TYPICAL MOMENT-CURVATURE RELATIONS FOR HAT SECTIONS

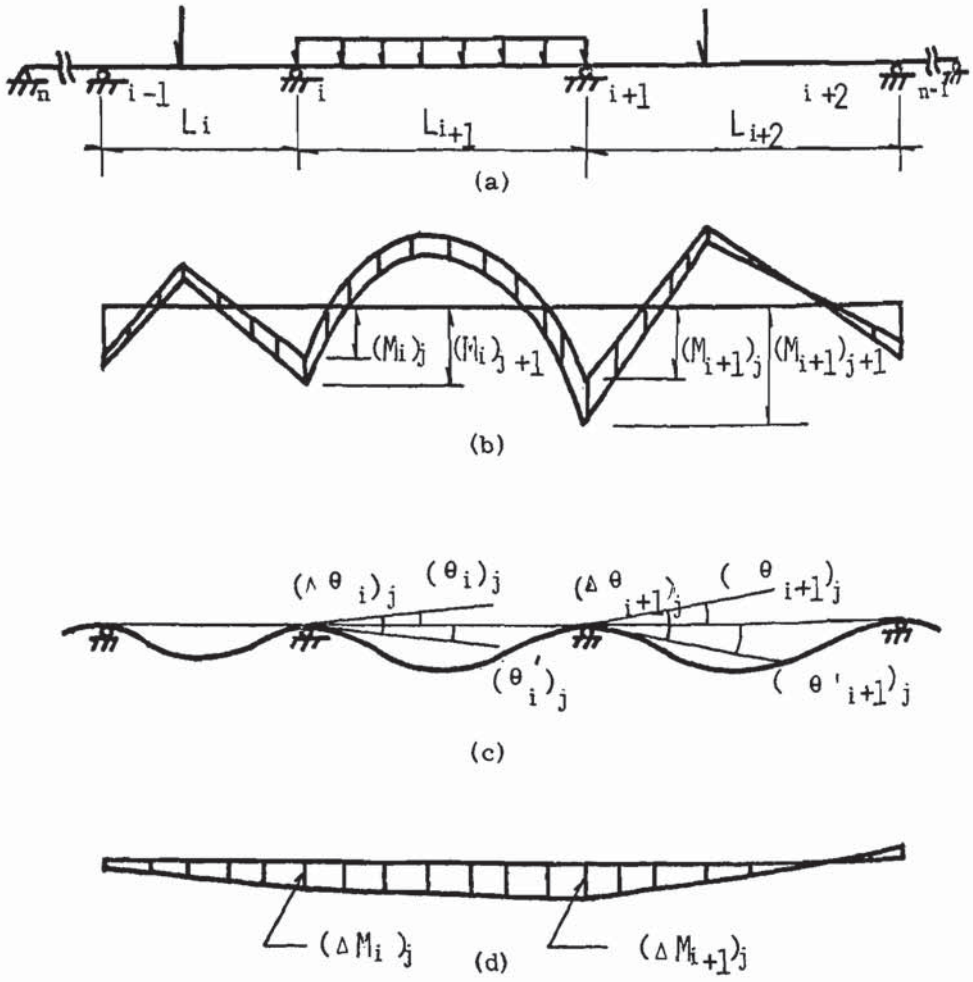

FIG. 4. - ITERATIVE PROCEDURE FOR POST-BUCKLING ANALYSIS

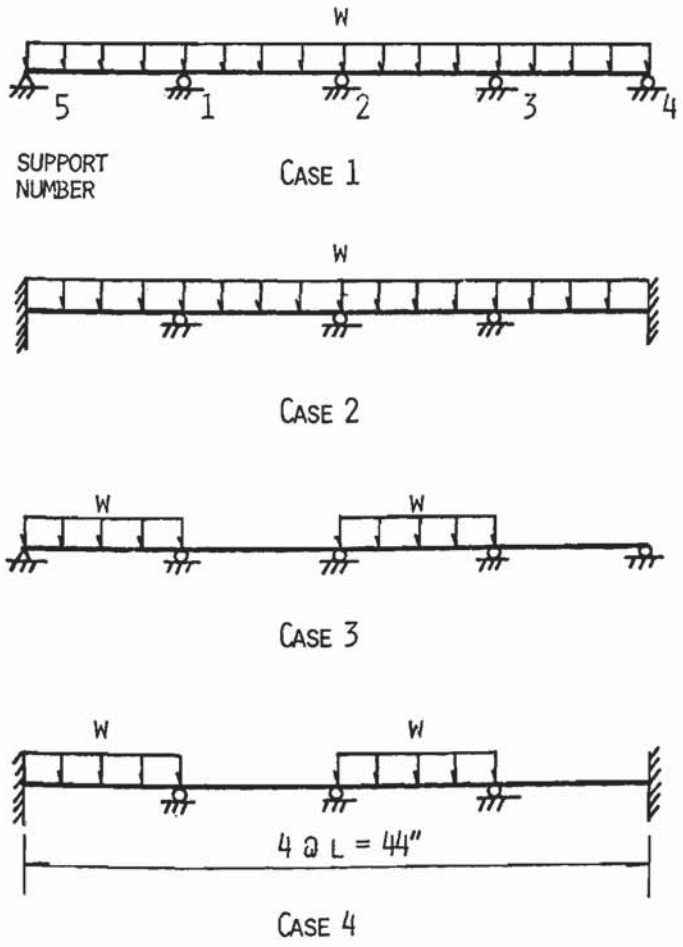

FIG. 5. - LOADING AND SUPPORT CONDITIONS

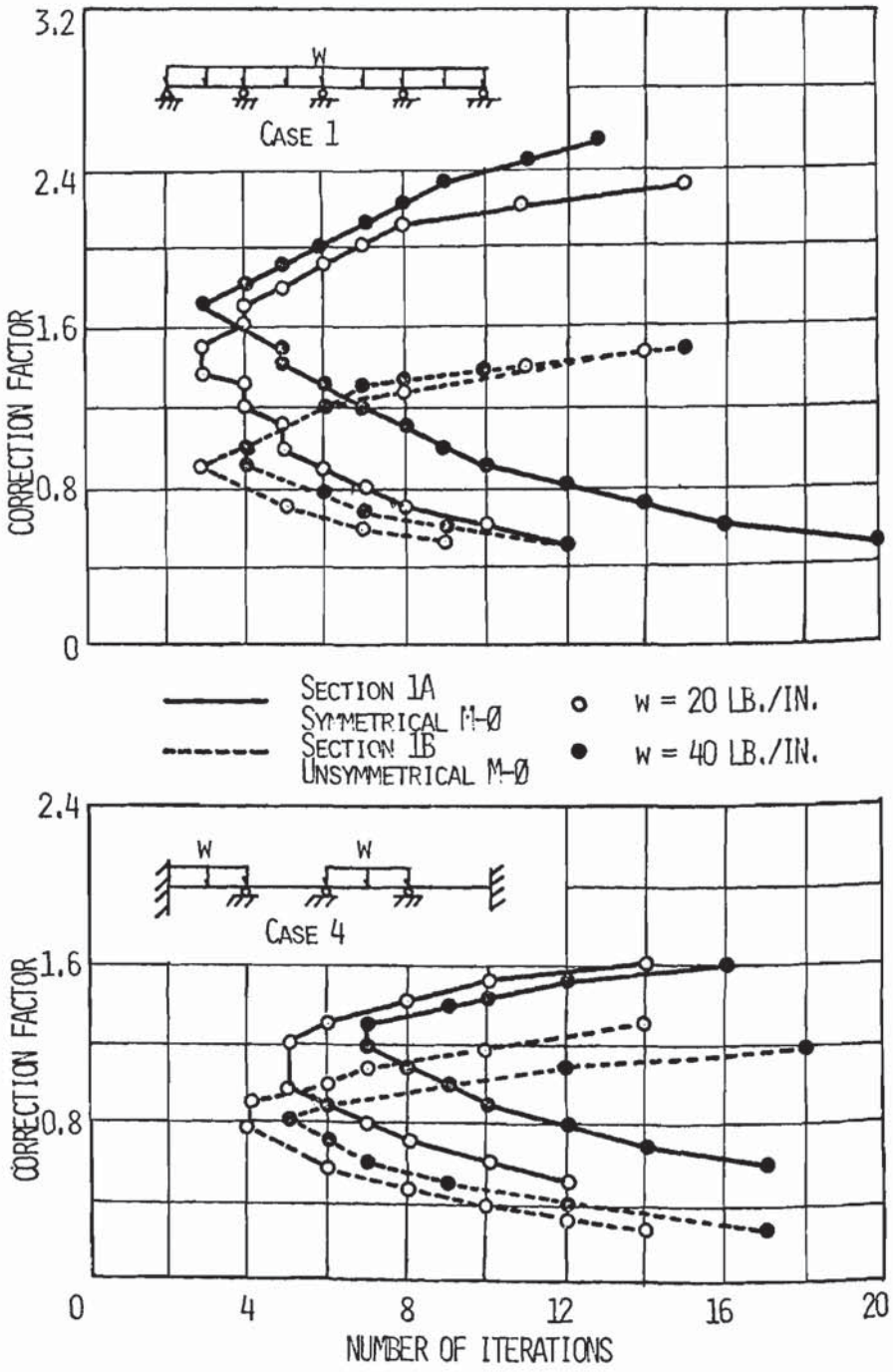

FIG. 6. - REQUIRED NUMBER OF ITERATIONS FOR CONVERGENCE AS A FUNCTION OF CORRECTION FACTOR

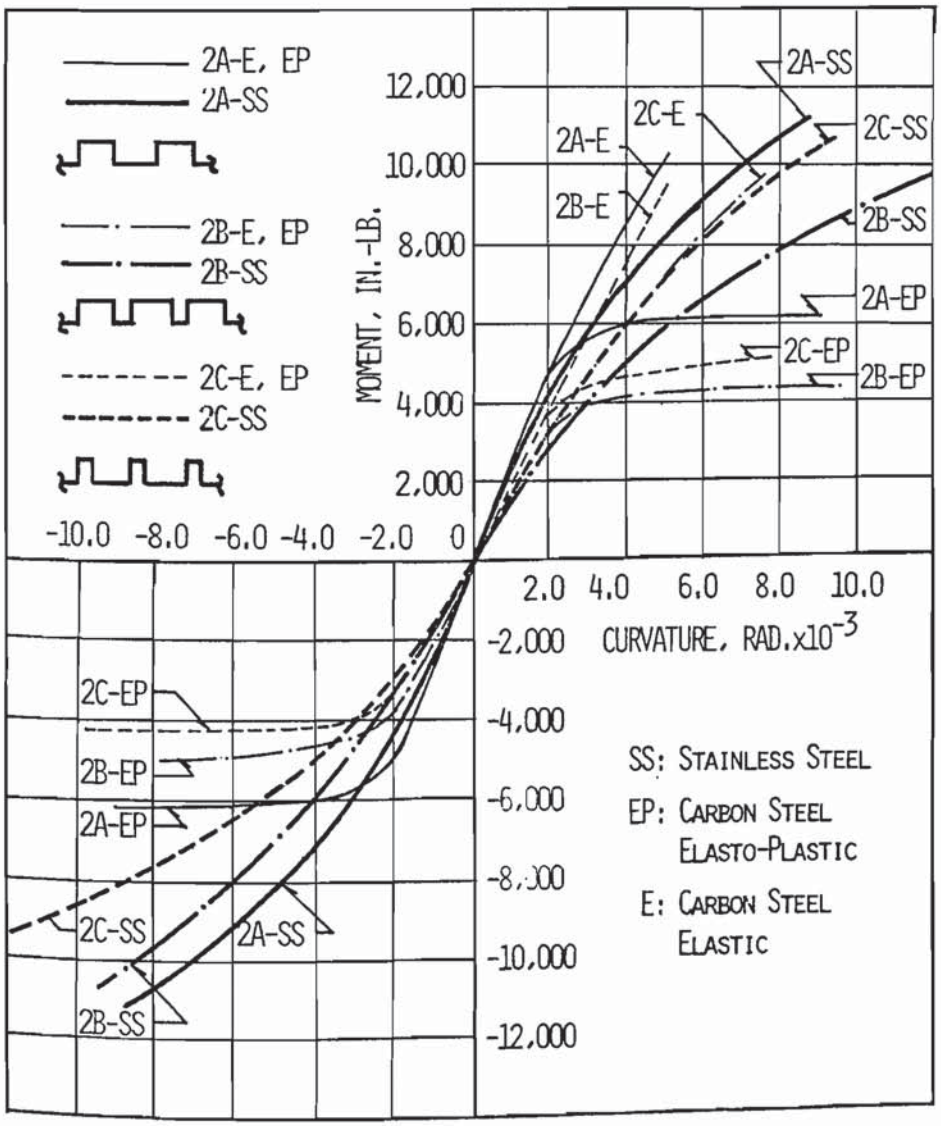

FIG. 7. - TYPICAL MOMENT-CURVATURE RELATIONS FOR CORRUGATED SECTIONS

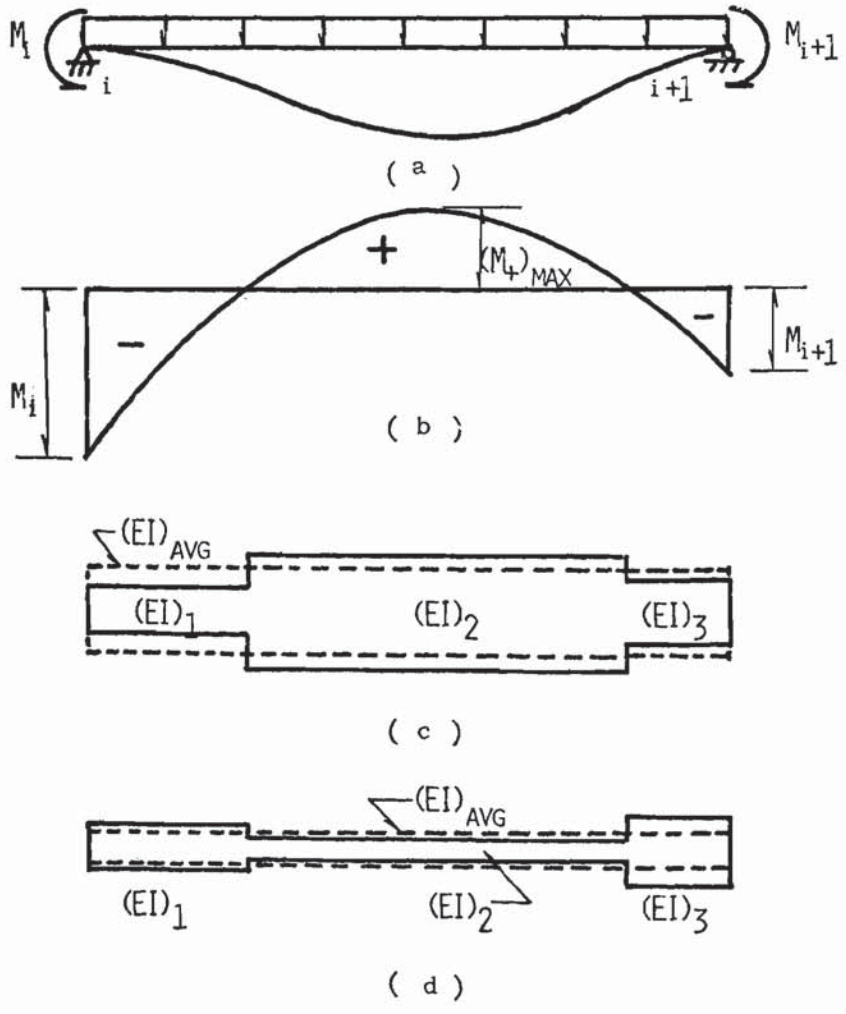

FIG. 8 - SIMPLIFIED METHODS FOR DEFLECTION CALCULATIONS